



## Human serum albumin nanoparticles for enhanced drug delivery to treat breast cancer: Preparation and *In Vitro* assessment

Ranjit Singh, C. Sankar and P. H. Rajasree

KMCH College of Pharmacy, Department of Pharmaceutics,  
Dr. M.G.R Medical University, Coimbatore (TN) - India

### Abstract

Most anticancer drugs are greatly limited by the serious side effects that they cause. Tamoxifen is toxic to cancer cells and used against breast cancer. However, it may lead to irreversible cardio toxicity, which could even result in congestive heart failure. It decreases white blood cells count with increased risk of infections, hair loss, nausea, vomiting, loss of appetite, mouth or lip sores, diarrhoea, no menstruation. In order to avoid these harmful side effects to the patients and to improve the therapeutic efficacy of tamoxifen, we developed tamoxifen loaded - chitosan enhanced human serum albumin (HSA) nanoparticles. HSA is the most abundant plasma protein (35-50 g/l human serum) with an average half life of 19 days. HSA is a very soluble globular monomeric proteins consisting of 585 amino acid residues and 35 cysteinyl residues. When HSA is broken down the amino acid will provide nutrition to peripheral tissues. These properties as well as its preferential uptake in tumor and flamed tissues, biodegradability and lack of toxicity make it an ideal candidate for drug delivery. The formed nanoparticles were 137 nm in size with a surface zeta potential of +15 mV, prepared using 30 µg of chitosan added per mg of HSA. Cytotoxicity was not observed with empty chitosan enhanced HSA nanoparticles, formed with low-molecular weight (250) kDa chitosan, indicating biocompatibility and safety of the nanoparticle formulation. Under optimized transfection conditions, approximately 80% of cells were transfected with HSA nanoparticles containing tetramethyl rhodamine-conjugated bovine serum albumin. Conclusively, chitosan enhanced HSA nanoparticles show potential for developing into an effective carrier for anticancer drugs.

Key-Words: Human serum albumin, Nanoparticles, Desolvation method, Cell viability, Breast cancer, Tamoxifen

### Introduction

Tamoxifen is a commonly used anti-cancer drug. It is most often used against breast cancer, carcinomas, osteosarcoma and soft-tissue sarcomas. The effectiveness of tamoxifen in treating various types of cancers is greatly limited by the serious side effects caused by the drug. The initial side effects caused as a result of tamoxifen administration include less serious symptoms, such as nausea, vomiting, myelo suppression, and arrhythmia, which are usually reversible<sup>1</sup>. However, tamoxifen associated cardiomyopathy and congestive heart failure have raised great concern among health practitioners<sup>2</sup>. A widely researched approach of increasing the efficacy, while lowering the deleterious side effects caused by anti-cancer agents such as tamoxifen, is of developing nanoparticles-based drug delivery systems<sup>3,5</sup>.

Various kinds of nanoparticles have been studied for the delivery of tamoxifen, which include poly (butylcyanoacrylate)<sup>6</sup>, poly (isohexylcyanoacrylate)<sup>7</sup>, poly(lactic-co-glycolic acid)<sup>8</sup>, chitosan<sup>9</sup>, gelatine<sup>10</sup>, and liposomes<sup>11</sup>. In addition, Dreis et al. employed human serum albumin (HSA) nanoparticles of a size range between 150 and 500 nm to deliver tamoxifen to a neuroblastoma cell line<sup>3</sup>. These nanoparticles showed a loading efficiency of 70-95% and an increased anti-cancer effect as compared to free tamoxifen. The endogenous HSA serves as a suitable material for nanoparticles formation as albumin is naturally found in the blood and is thus easily degraded, nontoxic, and nonimmunogenic<sup>12</sup>. Albumin is an acidic protein and remains stable between pH range 4-9 and temperatures up to 60° C. In addition, clinical studies carried out with HSA particle formulations, Alunex<sup>13</sup> and Abraxane<sup>14</sup>, have shown that albumin-based nanoparticles do not have any adverse effects on the body. Furthermore, albumin-based nanoparticles delivery systems are easily accumulated in tumor tissue

### \* Corresponding Author

E.mail: ranjitsingh08685@gmail.com  
Mob.: +91-9042978206

due to the enhanced permeability and retention (EPR) effect<sup>15,17</sup>. The vasculature in an active tumor is different from the vessels found in normal tissue. The distinctive tumor vasculature has the following properties: hypervascularity, poorly developed vascular architecture, a defective lymphatic drainage, and slow venous blood return<sup>15,16</sup>. These characteristics lead to the preferential accumulation and retention of macromolecules and nanoparticles in the tumor tissue. Therefore, using a nanoparticles delivery system to deliver low-molecular-weight anti-cancer drugs will be passively targeted to the tumour tissue through the EPR effect<sup>17</sup>. In addition, studies have also suggested that accumulation of albumin-based nanoparticles within the tumor tissue is also because of transcytosis, which occurs by the binding of albumin to 60-kDa glycoprotein (gp 60) receptor, which then results in the binding of gp 60 with caveolin-1 and the consequent formation of transcytotic vesicles<sup>12,18</sup>. Taking into consideration the factors mentioned above, HSA seems to be a suitable material to use for nanoparticles synthesis.

The surface properties of nanoparticles play a vital role in the cellular internalization of the particles. A neutrally charged surface does not show tendency of interacting with cell membranes, while charged groups found on nanoparticles are actively involved in nanomaterial-cell interaction<sup>19</sup>. Cho and Caruso found in their study of cellular internalization of gold nanoparticles that positively charged particles demonstrate greater adherence to the cell membrane and are thus taken up by the cells more than negatively and neutrally charged nanoparticles<sup>20</sup>. Cationic nanoparticles are shown to bind the negatively charged functional groups, such as sialic acid, found on cell surfaces and initiate translocation<sup>19</sup>. Due to the highly efficient transfection property of positively charged nanoparticles, many nanoparticles-based drug and gene delivery systems are positively charged. In this study, chitosan, a cationic polymer, has been used to coat the HSA nanoparticles in order to add stability and a positive surface charge to the nanoparticles. Chitosan may possess a linear or branched structure, with molecular weight ranging between 1 and 1000 kDa<sup>21</sup>. Chitosan has been observed to result in higher cellular uptake. The most commonly used stabilizing agent for the preparation of HSA nanoparticles, glutaraldehyde, has been reported to interfere with the release of the encapsulated material<sup>10, 23</sup>. Thus, chitosan is being employed as an alternative to glutaraldehyde in the current study.

In the current research study, the effectiveness of tamoxifen loaded -chitosan enhanced HSA

nanoparticles used against MCF-7 breast cancer cells was investigated. We prepared the nanoparticles using an ethanol desolvation method and characterized by measuring particle size, surface zeta potential, and cellular uptake<sup>22, 27, 28</sup>. The cytotoxicity of the developed tamoxifen loaded nanoparticles was assessed in comparison to free tamoxifen at varying drug concentrations over different time points. Results were promising and suggest that the study needs to be followed up with an in vivo investigation of the tamoxifen -loaded chitosan-enhanced HSA nanoparticles.

## **Material and Methods**

### **Materials**

Human serum albumin (HAS fractionV, Purity 96–99%), 8% glutaraldehyde, and chitosan were purchased from Sigma Aldrich (Canada). Tamoxifen was purchased from Urmilla chemopharma private limited (Mumbai). All other reagents were purchased from Fischer (Canada). Tetramethyl rhodamine-conjugated bovine serum albumin (BSA) was purchased from Invitrogen (Canada). To maintain the cell culture, the reagents such as fetal bovine serum, trypsin, Dulbecco's modified Eagle's Medium (DMEM), and Opti-MEM I Reduced Serum Medium were obtained from Invitrogen (Canada). The breast cancer cell line, MCF-7, was purchased from ATCC (Canada). Promega Cell-Titer 96A Queous Non-Radioactive Cell Proliferation MTS Assay kit was purchased from Promega (Wis, USA).

### **Preparation of Tamoxifen-Loaded chitosan-Enhanced HSA Nanoparticles**

Chitosan-coated HSA nanoparticles were prepared at room temperature using an ethanol desolvation technique<sup>22, 27–29</sup>. In brief, 20 mg of HSA was added to 1mL of 10mM NaCl (aq) under constant stirring (800 rpm) at room temperature. The solution was stirred for 10 min. After total dissolution, the solution was titrated to pH 8.5 with 1N NaOH (aq) and stirred for 5 min. This aqueous phase was desolvated by the dropwise addition of ethanol to aqueous HSA solution under constant stirring. Ethanol was added until the HSA solution became turbid (~12mL). Cross-linking agent, 8% glutaraldehyde, was added to form stable HSA particles. The obtained nanoparticles were centrifuged three times and washed with deionized water (dH2O), followed by resuspension in an equal volume of PBS. Chitosan dissolved in dH 20 was added to the nanoparticle preparation to allow chitosan to form an outer coating due to electrostatic binding. For the preparation of tamoxifen-loaded HSA nanoparticles, tamoxifen was added to 1ml HAS solution after pH adjustment and allowed to stir for 4 hrs, followed by



ethanol addition. To determine the drug encapsulation efficiency, an indirect method was employed as shown by Sebak et al.<sup>27</sup>. The unloaded drug was quantified by measuring the free drug found in the supernatant of the prepared drug-loaded nanoparticles, using a UV spectrophotometer. Using the amount of unloaded drug, the drug-loaded quantity was determined [Total drug added ( $\mu\text{g}$ ) - free drug]. The encapsulation efficiency was then calculated using the amount of drug loaded into the nanoparticles: amount of drug loaded ( $\mu\text{g}$ )/theoretical maximum drug loading ( $\mu\text{g}$ )<sup>8</sup>.

#### **Purification of chitosan-Enhanced HSA Nanoparticles**

Chitosan coated HSA nanoparticles were ultracentrifuged (16500) or 12 min and added to 10 mM NaCl (aq) by vortexing and ultrasonication (Branson 2510). This method was repeated thrice to ensure complete removal of impurities.

#### **Determining Particle Size and Surface Zeta Potential**

The particle size and zeta potential were measured by electrophoretic laser Doppler anemometry, using a zeta potential analyzer (Brookhaven Instruments Corporation, USA). The nanoparticles were diluted 1:15 with distilled water prior to measurement<sup>27</sup>.

#### **Surface Characterization of Chitosan-Enhanced HSA Nanoparticles**

The size and shape of the HSA nanoparticles were observed by transmission electron microscopy (TEM), using Philips CM200 200 kV TEM (Markham, Canada). The samples for TEM were prepared by ultracentrifuging the nanoparticles and washing with distilled water, followed by air drying the samples overnight to allow removal of moisture<sup>22,27, 29</sup>.

#### **Transfection of MCF-7 Breast Cancer Cells with chitosan Enhanced HSA Nanoparticles**

Prior to transfecting cells with nanoparticles, cells were washed with PBS and replenished with fresh serum-free DMEM. The chitosan-coated HSA nanoparticles were prepared using 5% of Rhodamine-tagged HSA. The nanoparticles were purified and added to the cells. After 8 hrs of incubation of cells at 37° C with the nanoparticles, the culture medium was replaced with fresh DMEM, containing 10% FBS. Under the fluorescence microscope (TE2000-U, Nikon; USA), pictures were taken to assess the levels of transfection. The percentage of transfected cells was calculated by using the average of the number of cells exhibiting fluorescence under five different fields of view.

#### **Cell Viability Assay**

The number of surviving cells was assessed using the Promega Cell-Titer 96 Aqueous Non-Radioactive Cell Proliferation MTS Assay kit. 3-(4,5-dimethylthiazol-2-

yl)-5-(3-carboxymethoxyphenyl)-2-(4-sulfophenyl)-2H-tetrazolium, (MTS), and phenazine methosulfate reagents were used. Live cells reduce MTS to form formazan, a compound soluble in tissue-culture media. The amount of formazan is proportional to the number of living cells and can be quantified by measuring the absorbance of formazan, using 1420-040 Victor3 Multilabel Counter (Perkin Elmer, USA) at 490 nm. The intensity of the color produced by formazan indicates the viability of cells. MCF-7 cells were seeded onto a 96-well plate (104 cells per well) 24 hrs before treatment. Cytotoxicity was measured at the predetermined time for each experiment using the MTS assay which was performed as per the manufacturer's protocol.

#### **Tunel Assay**

The DeadEnd Colorimetric TUNEL System detects DNA fragmentation (an indicator of apoptosis) of each cell undergoing apoptosis. The fragmented ends of DNA are labelled by a modified TUNEL (TdT-mediated dUTP Nick-End Labeling) assay. The terminal deoxynucleotidyl transferase (TdT) enzyme adds a biotinylated nucleotide at the 3'-OH ends of DNA; the biotinylated nucleotides are conjugated with horseradish-peroxidase-labeled streptavidin. The peroxidase is then detected using its substrate, hydrogen peroxide, and the chromogen, diaminobenzidine (DAB). Following the manufacturer's protocol, the nuclei of apoptotic cells are stained brown.

#### **Results and Discussion**

Increased Cellular Uptake of chitosan-Enhanced HSA Nanoparticles. The cellular internalization of chitosan-enhanced HSA nanoparticles was assessed by transfecting MCF-7 breast cancer cells with nanoparticles prepared with Rhodamine-tagged HSA. As shown in Figure 4, images were taken using a fluorescence microscope (TE2000-U, Nikon; USA). Cell transfection was measured with respect to the amount of chitosan added to coat the nanoparticles. It is essential to optimize the amount of chitosan used for coating the nanoparticles as this helps determine how much of the polymer is required to reach the maximum adsorption capacity of the surface of the nanoparticles and their corresponding surface zeta potential. Firstly, the lowest percentage of cell transfection was observed with uncoated nanoparticles, which can be attributed to the negative surface zeta potential of the uncoated HSA nanoparticles. Based on Fig. 4(a), it can be concluded that increasing the amount of chitosan, up to 30  $\mu\text{g}$  of chitosan per mg of HSA, used for coating the nanoparticles leads to an increase in cell transfection. Further increasing the amount of chitosan used for

coating the nanoparticles did not translate into higher transfection efficiency. This observation could be explained by reaching the maximum capacity of chitosan binding with the surface of HSA nanoparticles. Figures 4(b), 4(c), and 4(d) show corresponding fluorescence images of cellular uptake of chitosan-enhanced HSA nanoparticles. The increase in cell transfection due to coating the nanoparticles with chitosan is in agreement with previously published results. Cationic nanoparticles are shown to bind the negatively charged functional groups, such as sialic acid, found on cell surfaces and initiate transcytosis<sup>19</sup>. Chitosan-based nanoparticles have shown increased cellular uptake of siRNA. In vivo administration of siRNA delivered using chitosan-based nanoparticles resulted in 80% decrease in the target gene expression; however, cytotoxicity was a concern<sup>37,38</sup>. Therefore, a reasonable conclusion to draw from the results of the cell transfection experiment would be that the chitosan adsorbed to the surface of the nanoparticles aids in the internalization of the particles.

#### **Tamoxifen Delivery with Chitosan-Enhanced HSA Nanoparticles to Kill Breast Cancer Cells**

The efficacy of anti-cancer chemotherapy is limited by the cytotoxic effect on healthy cells due to a lack of selectivity of the drugs and poor uptake of the therapeutics by the tumor cells<sup>19, 39, 40</sup>. Tamoxifen has been shown to cause irreversible cardiomyopathy, which could also lead to congestive heart failure<sup>1,19,40</sup>. In order to overcome this issue, many researchers have tried delivering tamoxifen by nanoparticles that reduce the amount of drug reaching cardiac tissue while increasing the accumulation of the drug-loaded nanoparticles in the tumor tissue<sup>7, 9, 32,41-43</sup>. Furthermore, by incorporating a layer of chitosan on the surface of the HSA nanoparticles, we aimed to increase their cellular uptake in the tumor tissue. Previously, uncoated HSA nanoparticles were studied for the delivery of tamoxifen to neuroblastoma cell lines. Results suggested that tamoxifen delivered using nanoparticles was more cytotoxic against cancer cells as compared to free tamoxifen. In our study, we observed that the cytotoxicity of tamoxifen-loaded nanoparticles and free tamoxifen against MCF-7 breast cancer cells was about the same after 48 hrs as the tamoxifen concentration was increased. However, assessing the cytotoxicity at different time points showed that tamoxifen-loaded nanoparticles led to a greater decrease in cell viability as compared to free tamoxifen after 144 hrs. This observation can be explained by the slow release of tamoxifen from the nanoparticles. These results would be more effective in

vivo as the free drug would diffuse out of the tumor tissue, while the nanoparticles would accumulate within the tumor tissue due to the EPR effect and release the drug over time. Images of treated cells after TUNEL staining in Figures 3(a), 3(b), and 3(c) confirm that the cytotoxic effect of tamoxifen-loaded nanoparticles was comparable to free tamoxifen. Figure 3(c) shows that the cells remained healthy and viable after the addition of chitosan-enhanced HSA nanoparticles, suggesting that the nanoparticles formulation does not have cytotoxic effects

#### **Conclusion**

In our current study, we used modified HSA nanoparticles by adding an outer coating of the chitosan to improve the therapeutic index of tamoxifen against MCF-7 breast cancer cells. The nanoparticles prepared were characterized based upon size and surface charge with respect to the amount of chitosan used for coating. A rise in the surface zeta potential of the nanoparticles confirms the electrostatic binding of chitosan with the surface of HSA nanoparticles. Different microscopic techniques were employed to observe the shape, dispersion, and morphology of the nanoparticles. Chitosan-enhanced HSA nanoparticles resulted in a higher cell transfection percentage, indicating that the addition of the layer of cationic polymer did improve cell penetration of the particles. Chitosan-enhanced HSA nanoparticles illustrated a more potent cytotoxic effect on MCF-7 breast cancer cells over longer time duration. The results shown in this study are promising and set a platform for further examining the suitability of this chitosan-enhanced delivery system in vivo.

#### **Conclusion**

The authors are thankful to The Principal Dr. A. Rajasekaran, KMCH College of Pharmacy for providing the necessary facilities in the Colleges. Sincerely thanks to Dr. C. Sankar, Professor Department of Pharmacuetics, KMCH College of Pharmacy, Kovai Estate, Coimbatore - 35, Tamil Nadu (INDIA) for his valuable support. We would also like to thank our colleagues, lab assistants for their support.

#### **References**

1. P. K. Singal and N. Iliskovic, "Doxorubicin-induced cardiomyopathy," *The New England Journal of Medicine*, vol. 339, no. 13,
2. P. K. Singal, T. Li, D. Kumar, I. Danelisen, and N. Iliskovic, "Adriamycin-induced heart failure: mechanism and modulation," *Molecular and Cellular Biochemistry*, vol. 207, no. 1-2, pp. 77-85, 2000.
3. Dreis, F. Rothweiler, M. Michaelis, J. Cinatl, J. Kreuter, and K. Langer, "Preparation,



- characterisation and maintenance of drug efficacy of doxorubicin-loaded human serum albumin (HSA) nanoparticles,” *International Journal of Pharmaceutics*, vol. 341, no. 1-2, pp. 207–214, 2007.
4. M. L. Hans and A. M. Lowman, “Biodegradable nanoparticles for drug delivery and targeting,” *Current Opinion in Solid State and Materials Science*, vol. 6, no. 4, pp. 319–327, 2002.
  5. R. Seigneuric, L. Markey, D. S. A. Nuyten et al., “From nanotechnology to nanomedicine: applications to cancer research,” *Current Molecular Medicine*, vol. 10, no. 7, pp. 640–652, 2010.
  6. E. Gulyaev, S. E. Gelperina, I. N. Skidan, A. S. Antropov, G. Y. Kivman, and J. Kreuter, “Significant transport of doxorubicin into the brain with polysorbate 80-coated nanoparticles,” *Pharmaceutical Research*, vol. 16, no. 10, pp. 1564–1569, 1999.
  7. Cuvier, L. Roblot-Treupel, J. M. Millot et al., “Doxorubicin-loaded nanospheres bypass tumor cell multidrug resistance,” *Biochemical Pharmacology*, vol. 44, no. 3, pp. 509–517, 1992.
  8. J. Park, P. M. Fong, J. Lu et al., “PEGylated PLGA nanoparticles for the improved delivery of doxorubicin,” *Nanomedicine: Nanotechnology, Biology, and Medicine*, vol. 5, no. 4, pp. 410–418, 2009.
  9. K. A. Janes, M. P. Fresneau, A. Marazuela, A. Fabra, and M. J. Alonso, “Chitosan nanoparticles as delivery systems for doxorubicin,” *Journal of Controlled Release*, vol. 73, no. 2-3, pp. 255–267, 2001.
  10. E. Leo, M. A. Vandelli, R. Camerini, and F. Forni, “Doxorubicin-loaded gelatin nanoparticles stabilized by glutaraldehyde: involvement of the drug in the cross-linking process,” *International Journal of Pharmaceutics*, vol. 155, no. 1, pp. 75–82, 1997.
  11. N. Lukyanov, T. A. Elbayoumi, A. R. Chakilam, and V. P. Torchilin, “Tumor-targeted liposomes: doxorubicin-loaded long-circulating liposomes modified with anti-cancer anti-body,” *Journal of Controlled Release*, vol. 100, no. 1, pp. 135–144, 2004.
  12. F. Kratz, “Albumin as a drug carrier: design of prodrugs, drug conjugates and nanoparticles,” *Journal of Controlled Release*, vol. 132, no. 3, pp. 171–183, 2008.
  13. S. B. Feinstein, J. Cheirif, F. J. Ten Cate et al., “Safety and efficacy of a new transpulmonary ultrasound contrast agent: initial multicenter clinical results,” *Journal of the American College of Cardiology*, vol. 16, no. 2, pp. 316–324, 1990.
  14. N. K. Ibrahim, N. Desai, S. Legha et al., “Phase I and pharmacokinetic study of ABI-007, a Cremophor-free, protein-stabilized, nanoparticle formulation of paclitaxel,” *Clinical Cancer Research*, vol. 8, no. 5, pp. 1038–1044, 2002.
  15. H. Maeda, J. Wu, T. Sawa, Y. Matsumura, and K. Hori, “Tumor vascular permeability and the EPR effect in macromolecular therapeutics: a review,” *Journal of Controlled Release*, vol. 65, no. 1-2, pp. 271–284, 2000.
  16. H. Maeda, “Tumor-selective delivery of macromolecular drugs via the EPR effect: background and future prospects,” *Bioconjugate Chemistry*, vol. 21, no. 5, pp. 797–802, 2010.
  17. Y. J. Son, J. S. Jang, Y. W. Cho et al., “Biodistribution and anti-tumor efficacy of doxorubicin loaded glycol-chitosan nanoaggregates by EPR effect,” *Journal of Controlled Release*, vol. 91, no. 1-2, pp. 135–145, 2003.
  18. N. Desai, V. Trieu, Z. Yao et al., “Increased antitumor activity, intratumor paclitaxel concentrations, and endothelial cell transport of cremophor-free, albumin-bound paclitaxel, ABI-15, pp. 8786–8791, 2001.007, compared with cremophor-based paclitaxel,” *Clinical Cancer Research*, vol. 12, no. 4, pp. 1317–1324, 2006.
  19. Verma and F. Stellacci, “Effect of surface properties on nanoparticle-cell interactions,” *Small*, vol. 6, no. 1, pp. 12–21,
  20. J. Cho and F. Caruso, “Investigation of the interactions between ligand-stabilized gold nanoparticles and polyelectrolyte multilayer films,” *Chemistry of Materials*, vol. 17, no. 17,
  21. Kichler, “Gene transfer with modified polyethylenimines,” *Journal of Gene Medicine*, vol. 6, no. 1, pp. S3–S10, 2004.
  22. S. Abbasi, A. Paul, and S. Prakash, “Investigation of siRNA-loaded polyethylenimine-coated human serum albumin nanoparticle complexes for the

- treatment of breast cancer," *Cell Biochemistry and Biophysics*. In press.
23. S. Segura, S. Espuelas, M. J. Renedo, and J. M. Irache, "Potential of albumin nanoparticles as carriers for interferon gamma," *Drug Development and Industrial Pharmacy*, vol. 31, no. 3, pp. 271–280, 2005.
  24. G. Wang, K. Siggers, S. Zhang et al., "Preparation of BMP-2 containing bovine serum albumin (BSA) nanoparticles stabilized by polymer coating," *Pharmaceutical Research*, vol. 25, no. 12, pp. 2896–2909, 2008.
  25. S. Zhang, G. Wang, X. Lin et al., "Polyethylenimine-coated albumin nanoparticles for BMP-2 delivery," *Biotechnology Progress*, vol. 24, no. 4, pp. 945–956, 2008.
  26. S. Zhang, M. R. Doschak, and H. Uludağ, "Pharmacokinetics and bone formation by BMP-2 entrapped in poly ethylenimine-coated albumin nanoparticles," *Biomaterials*, vol. 30, no. 28, pp. 5143–5155, 2009.
  27. S. Sebak, M. Mirzaei, M. Malhotra, A. Kulamarva, and S. Prakash, "Human serum albumin nanoparticles as an efficient noscapine drug delivery system for potential use in breast cancer: preparation and in vitro analysis," *International Journal of Nanomedicine*, vol. 5, no. 1, pp. 525–532, 2010.
  28. C. Weber, J. Kreuter, and K. Langer, "Desolvation process and surface characteristics of HSA-nanoparticles," *International Journal of Pharmaceutics*, vol. 196, no. 2, pp. 197–200, 2000.
  29. K. Langer, S. Balthasar, V. Vogel, N. Dinauer, H. Von Briesen, and D. Schubert, "Optimization of the preparation process for human serum albumin (HSA) nanoparticles," *International Journal of Pharmaceutics*, vol. 257, no. 1-2, pp. 169–180, 2003.
  30. Khan, A. Paul, S. Abbasi, and S. Prakash, "Mitotic and antiapoptotic effects of nanoparticles coencapsulating human VEGF and human angiopoietin 1 on vascular endothelial cells," *International Journal of Nanomedicine*, vol. 6, no. 1, pp. 1–10, 2011.
  31. F.M. Menger and B. M. Sykes, "Anatomy of a coacervate," *Research*, vol. 8, no. 5, pp. 1038–1044, 2002. *Langmuir*, vol. 14, no. 15, pp. 4131–4137, 1998.
  32. W. Lin, A. G. Coombes, M. C. Davies, S. S. Davis, and L. Illum, "Preparation of sub-100 nm human serum albumin nanospheres using a pH-coacervation method," *Journal of Drug Targeting*, vol. 1, no. 3, pp. 237–243, 1993.
  33. H. D. Singh, G. Wang, H. Uludağ, and L. D. Unsworth, "Poly- L-lysine-coated albumin nanoparticles: stability, mechanism for increasing in vitro enzymatic resilience, and siRNA release characteristics," *Acta Biomaterialia*, vol. 6, no. 11, pp. 4277–4284, 2010.
  34. V. P. Torchilin, R. Rammohan, V. Weissig, and T. S. Levchenko, "TAT peptide on the surface of liposomes affords their efficient intracellular delivery even at low temperature and in the presence of metabolic inhibitors," *Proceedings of the National Academy of Sciences of the United States of America*, vol. 98, no. 15, pp. 8786–8791, 2001.
  35. S. Prabha, W. Z. Zhou, J. Panyam, and V. Labhasetwar, "Size dependency of nanoparticle-mediated gene transfection: studies with fractionated nanoparticles," *International Journal of Pharmaceutics*, vol. 244, no. 1-2, pp. 105–115, 2002.
  36. O. Harush-Frenkel, E. Rozentur, S. Benita, and Y. Altschuler, "Surface charge of nanoparticles determines their endocytic and transcytotic pathway in polarized MDCK cells," *Biomacromolecules*, vol. 9, no. 2, pp. 435–443, 2008.
  37. C. Hunter, "Molecular hurdles in polyfectin design and mechanistic background to polycation induced cytotoxicity," *Advanced Drug Delivery Reviews*, vol. 58, no. 14, pp. 1523–1531, 2006.
  38. N. Tietze, J. Pelisek, A. Philipp et al., "Induction of apoptosis in murine neuroblastoma by systemic delivery of transferrin shielded siRNA polyplexes for downregulation of Ran," *Oligonucleotides*, vol. 18, no. 2, pp. 161–174, 2008.
  39. K. L. Maughan, M. A. Lutterbie, and P. S. Ham, "Treatment of breast cancer," *American Family Physician*, vol. 81, no. 11, pp. 1339–1346, 2010.
  40. H. Partridge, H. J. Burstein, and E. P. Winer, "Side effects of chemotherapy and combined chemohormonal therapy in women with early-stage breast cancer," *Journal of the National Cancer Institute. Monographs*, no. 30, pp. 135–142, 2001.
  41. S. Bennis, C. Chapey, P. Couvreur, and J. Robert, "Enhanced cytotoxicity of doxorubicin encapsulated in polyisohexylcyanoacrylate



- nanospheres against multidrug-resistant tumour cells in culture,” *European Journal of Cancer Part A*, vol. 30, no. 1, pp. 89–93, 1994.
42. L. Brannon-Peppas and J. O. Blanchette, “Nanoparticle and targeted systems for cancer therapy,” *Advanced Drug Delivery Reviews*, vol. 56, no. 11, pp. 1649–1659, 2004.
43. R. Dhankhar, S. P. Vyas, A. K. Jain, S. Arora, G. Rath, and A. K. Goyal, “Advances in novel drug delivery strategies for breast cancer therapy,” *Artificial Cells, Blood Substitutes, and Biotechnology*, vol. 38, no. 5, pp. 230–249, 2010.

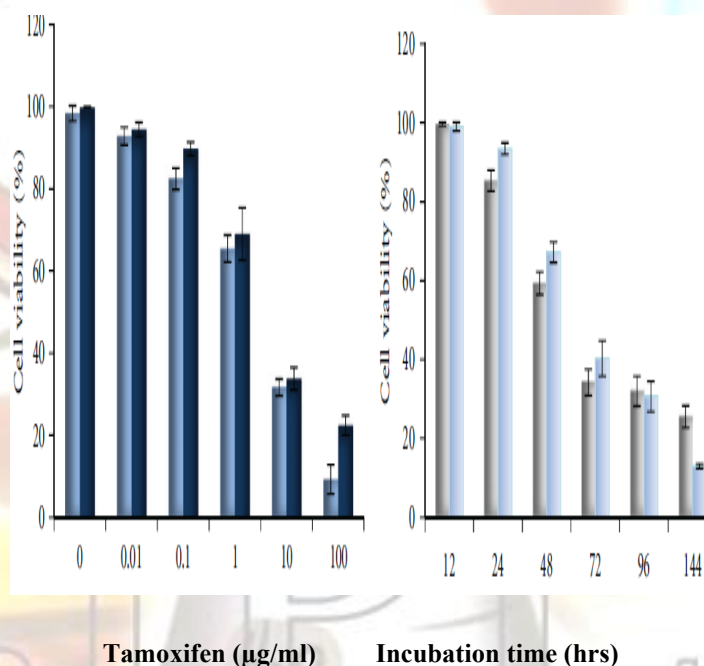
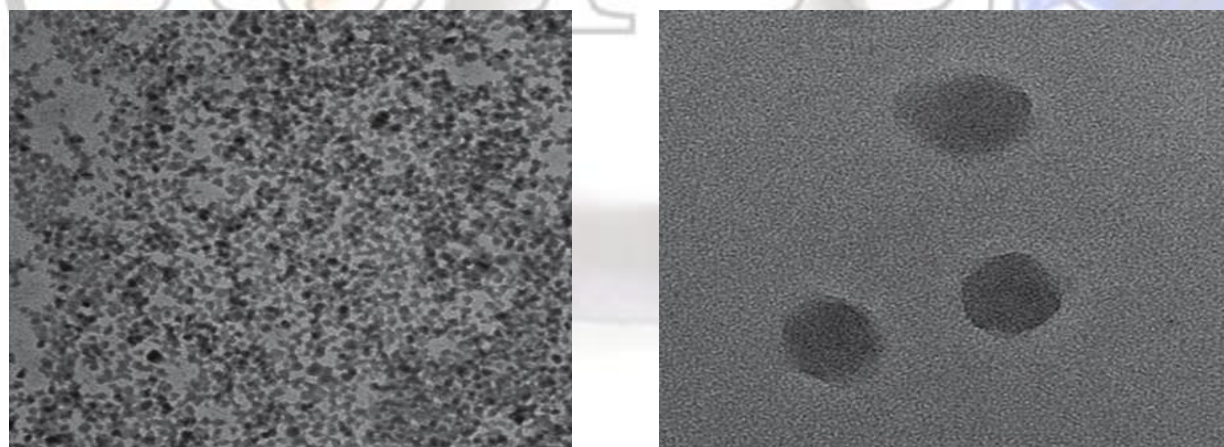


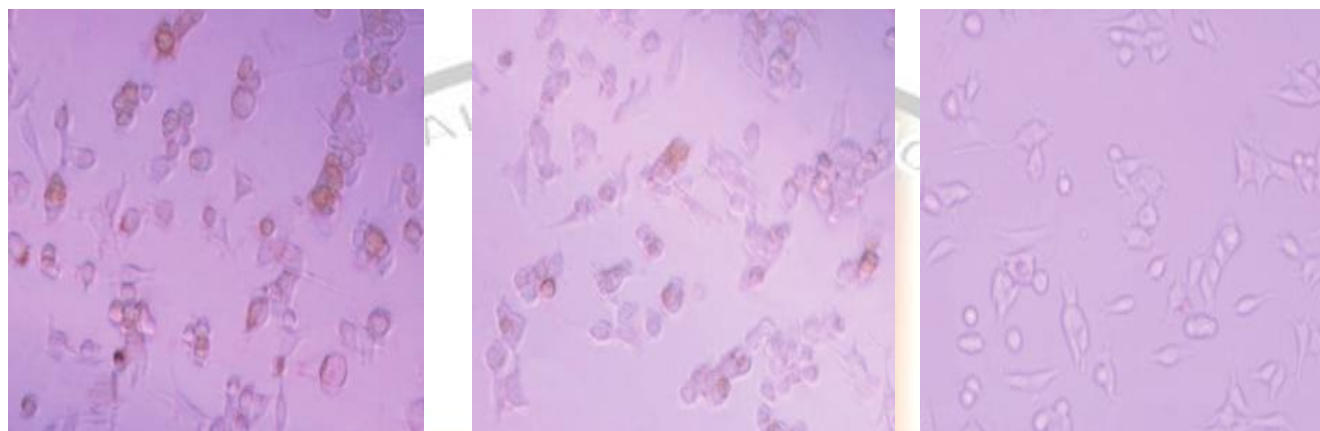
**Fig. 1: Dose response cytotoxicity of nanoparticles**



**(a) 500 nm**

**(b) 200 nm**

**Fig. 2: (a) Transmission electron microscope images of drug-loaded chitosan-enhanced HSA nanoparticles. (b) Higher magnification image of the nanoparticles**

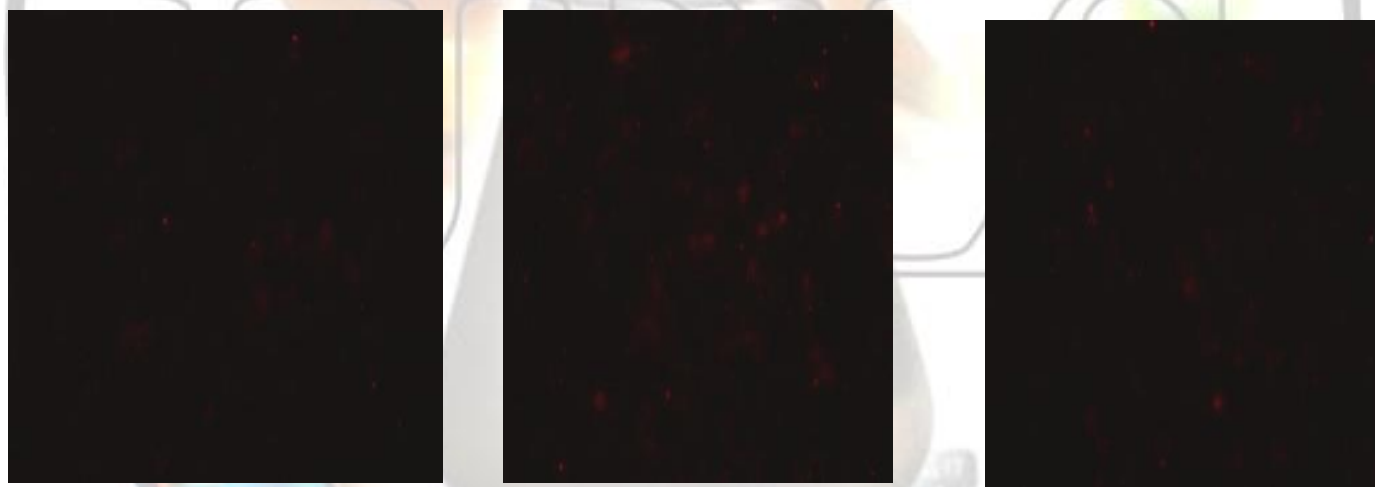


(a) 100  $\mu$ m

(b) 100  $\mu$ m

(c) 100  $\mu$ m

**Fig. 3: TUNEL assay to confirm cell death after tamoxifen administration (24 hrs): (a) tamoxifen -loaded chitosan-enhanced HSA nanoparticles, (b) free tamoxifen and (c) empty chitosan-enhanced HSA nanoparticles. The concentration of tamoxifen administered was 1  $\mu$ g/mL to MCF-7 breast cancer cells grown in 96 well plates.**



(a)

(b)

(c)



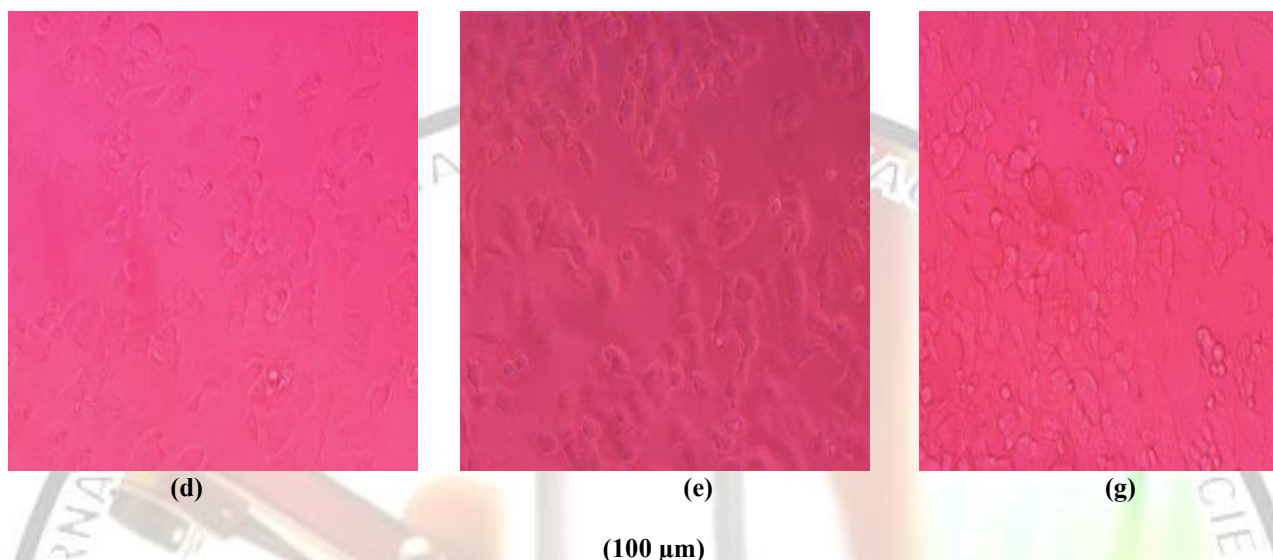


Fig. 4: Cellular uptake of chitosan-enhanced nanoparticles was assessed with respect to different amounts of chitosan used for coating (mean  $\pm$  S.D.,  $n = 3$ ). The cellular uptake was observed under a fluorescence microscope (TE2000-U, Nikon; USA). (a) Percentage of cellular uptake with nanoparticles prepared using 0, 10, 20, and 30  $\mu$ g of chitosan per mg of HSA. Varying quantities of nanoparticle preparations were added to the cells: 50, 100, and 200  $\mu$ l. Fluorescence images of cellular uptake of different HSA nanoparticle preparations, consisting of tetramethyl rhodamine-conjugated BSA, are shown; (b) uncoated HSA nanoparticles, (c) 10  $\mu$ g and (d) 30  $\mu$ g of chitosan added per mg of HSA to form chitosan-enhanced HSA nanoparticles. Corresponding bright field images are illustrated below (e, f, and g).

Table 1: Effect of the amount of chitosan added ( $\mu$ g per mg of HAS) on the physical characteristics of drug loaded chitosan enhanced HAS nanoparticles prepared at pH 8.5, 20 mg/ml HAS (mean  $\pm$  S.D,  $n=3$ )

Amount of chitosan ( $\mu$ g) added per mg of HSA	Particle size (nm)	Zeta potential (mV)
0	94.01 $\pm$ 2.01	- 44.3 $\pm$ 4.22
10	101.3 $\pm$ 4.73	+ 6.01 $\pm$ 1.6
20	118.6 $\pm$ 6.1	+ 11.7 $\pm$ 0.14
30	130.1 $\pm$ 2.41	+ 15.28 $\pm$ 1.11
40	129.23 $\pm$ 1.2	+ 16.24 $\pm$ 3.12

Table 2. Effect of incubation time for chitosan coating and stirring speed during the desolvation step on the physical characteristics of drug loaded chitosan enhanced HAS nanoparticles, prepared with 20 mg/ml HAS and 30  $\mu$ g of chitosan per of HAS (mean  $\pm$  S.D,  $n=30$ )

Time of incubation with chitosan (hrs)	Stirring speed (rpm)	Particle size (nm)	Zeta potential (mV)
4	250	404.21 $\pm$ 10.4	7.8 $\pm$ 0.14
	500	239.34 $\pm$ 3.1	7.20 $\pm$ 0.6
	1000	125.37 $\pm$ 9.6	3.42 $\pm$ 0.01
8	250	367.14 $\pm$ 0.31	16.36 $\pm$ 0.4
	500	210.75 $\pm$ 14.5	17.51 $\pm$ 0.26
	1000	110.43 $\pm$ 12.8	16.51 $\pm$ 0.39
12	250	326.76 $\pm$ 2.27	15.31 $\pm$ 0.19
	500	210.16 $\pm$ 6.18	11.71 $\pm$ 0.99
	1000	114.35 $\pm$ 7.42	12.37 $\pm$ 0.63